Inorg. Chem. **2006**, *45*, 3932–3940

Structure and Magnetism of $[M_3]^{6/7+}$ Metal Chain Complexes from Density Functional Theory: Analysis for Copper and Predictions for Silver

M. Bénard,[†] J. F. Berry,[‡,||] F. A. Cotton,[‡] C. Gaudin,[†] X. López,[†] C. A. Murillo,[‡] and M.-M. Rohmer*[,†]

Laboratoire de Chimie Quantique, UMR 7551, CNRS and Université Louis Pasteur, Strasbourg, France, and the Laboratory for Molecular Structure and Bonding, Department of Chemistry, Texas A&M University, P.O. Box 30012, College Station, Texas 77842-3012

Received October 18, 2005

The ground-state electronic structure of the trinuclear complex $Cu_3(dpa)_4Cl_2$ (**1**), where dpa is the anion of di(2-pyridyl)amine, has been investigated within the framework of density functional theory (DFT) and compared with that obtained for other known $M_3(dpa)_4Cl_2$ complexes (M = Cr, Co, Ni) and for the still hypothetical $Ag_3(dpa)_4Cl_2$ compound. Both coinage metal compounds display three singly occupied x^2-y^2-like (δ) orbitals oriented toward the nitrogen environment of each metal atom, generating antibonding M–(N_4) interactions. All other metal orbital combinations are doubly occupied, resulting in no delocalized metal–metal bonding. This is at variance with the other known symmetric $M_3(dpa)_4Cl_2$ complexes of the first transition series, which all display some delocalized bonding through the metal backbone, with formal bond multiplicity decreasing in the order Cr > Co > Ni. An antiferromagnetic coupling develops between the singly occupied MOs via a superexchange mechanism involving the bridging dpa ligands. This magnetic interaction can be considered as an extension to the three aligned Cu^{II} atoms of the well-documented exchange coupling observed in carboxylato-bridged dinuclear copper compounds. Broken-symmetry calculations with approximate spin projection adequately reproduce the coupling constant observed for **1**. Oxidation of **1** removes an electron from the magnetic orbital located on the central Cu atom and its ligand environment; $\mathbf{1}^+$ displays a much weaker antiferromagnetic interaction coupling the terminal Cu–N_4 moieties via four ligand pathways converging through the x^2-y^2 orbital of the central metal. The silver homologues of **1** and $\mathbf{1}^+$ display similar electronic ground states, but the calculated magnetic couplings are stronger by factors of about 3 and 4, respectively, resulting from a better overlap between the metal centers and their equatorial ligand environment within the magnetic orbitals.

Introduction

Recurrent interest for linear multinuclear string complexes is assigned to their versatile chemical and physical properties and to their potential applications as molecular metal wires.[1,2] Since the first reports on the trinuclear nickel and copper complexes,[3,4] a systematic effort has been made either to concatenate ligand-bridged dimetal precursors through unsupported metal−metal bonds[5−7] or to constrain a specific number of metal atoms to align by means of purposely designed ligands.[8−15] The latter approach has been particularly successful, mainly because of the synthesis of polypyridylamides, a family of *p*-dentate ligands with general

* To whom correspondence should be addressed. E-mail: rohmer@quantix.u-strasbg.fr.
† CNRS and Université Louis Pasteur.
‡ Texas A&M University.
|| Present Address: Max-Planck Institut für Bioanorganische Chemie, D-45470 Mülheim/Ruhr, Germany.

(1) Berry, J. F. In *Multiple Bonds between Metal Atoms*, 3rd ed.; Cotton, F. A., Murillo, C. A., Walton, R. A., Eds; Springer-Science and Business Media, Inc.: New York, 2005.
(2) Bera, J. K.; Dunbar, K. R. *Angew. Chem., Int. Ed.* **2002**, *41*, 4453.
(3) Aduldecha, S.; Hathaway, B. *J. Chem. Soc., Dalton Trans.* **1991**, 993.
(4) (a) Wu, L.-P.; Field, P.; Morrissey, T.; Murphy, C.; Nagle, P.; Hathaway, B.; Simmons, C.; Thornton, P. *J. Chem. Soc., Dalton Trans.* **1990**, 3835. (b) Pyrka, G. J.; El-Mekki, M.; Pinkerton, A. A. *J. Chem. Soc., Chem. Commun.* **1991**, 84.
(5) (a) Matsumoto, K.; Sakai, K. *Adv. Inorg. Chem.* **2000**, *49*, 375. (b) Matsumoto, K.; Sakai, K.; Nishio, K.; Tokisue, Y.; Ito, R.; Nishide, T.; Shichi, Y. *J. Am. Chem. Soc.* **1992**, *114*, 8110.
(6) (a) Miskowski, V. M.; Sigal, I. S.; Mann, K. R.; Gray, H. B.; Milder, S. J.; Hammond, G. S.; Ryason, P. R. *J. Am. Chem. Soc.* **1979**, *101*, 4384. (b) Sigal, I. S.; Mann, K. R.; Gray, H. B. *J. Am. Chem. Soc.* **1980**, *102*, 3965. (c) Mann, K. R.; DiPierro, M. J.; Gill, T. P. *J. Am. Chem. Soc.* **1980**, *102*, 3965.

10.1021/ic051799o CCC: $33.50
Published on Web 04/18/2006

formula $[C_5H_4N\text{-}(N\text{-}C_5H_3N)_n\text{-}N\text{-}C_5H_4N]^{(n+1)-}$ and $p = 2n + 3$.[9] On one hand, a variety of trinuclear complexes has been characterized and extensively studied with the tridentate dipyridylamide ligand or closely related variants,[10] associated with several types of axial ligands and with a large range of metals belonging to the first or second transition series (M = Co, Cr, Ni, Cu, Ru, Rh).[1,2] On the other hand, longer chains with 4, 5, 7, and up to 9 metal atoms, mainly chromium, cobalt, and nickel, could be assembled via the higher members of the polypyridylamide family.[1] Quite recently, a relative estimate of the electron-transfer intensity through the metal backbone of such nanowires composed of 3 or 5 atoms of Cr^{II}, Co^{II}, or Ni^{II}, surrounded with four appropriate polypyridylamide anions and completed with two NCS ligands in the axial position could be obtained by means of scanning tunneling microscopy (STM).[16] The values obtained with the neutral complexes were found to differ significantly according to the nature of the transition metal, and these discrepancies were correlated with a tentative scheme of electron localization−delocalization among the metal centers.[17] In this class of molecules, the arrangement of the four multidentate ligands constrains the atoms in the metal framework to remain at bonding distance from each other, typically between 2.25 and 2.6 Å, the variations induced by the metal−metal interaction or the lack thereof being confined in this relatively narrow range. As a consequence of this specificity and of the plurality of transition metal atoms that can be lined up in the complex core, these molecules and the associated oxidized species display a wide variety of distinctive structural features, some of them unprecedented. The most unusual case resides in the characterization of two different crystal networks for $Co_3(dpa)_4Cl_2$, associated with distinct molecular structures differing only in the length of the metal−metal and some metal−nitrogen bonds.[12]

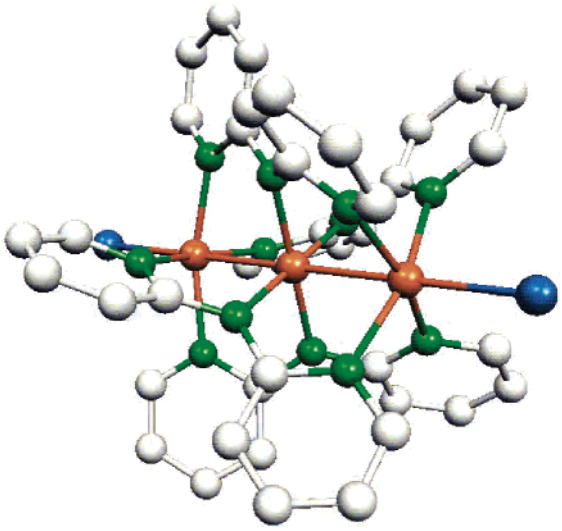

Figure 1. MOLDEN representation of a symmetric $M_3(dpa)_4Cl_2$ complex (orange, metal; blue, chlorine; green, nitrogen; white, carbon).

The goal of the present work is therefore to complete the DFT analysis of the bonding in symmetric $M_3(dpa)_4Cl_2$ systems (Figure 1), previously initiated for M = Co,[18] Cr,[19] and Ni,[20] for copper and to attempt a first approach to the trinuclear complexes of the second transition row by a comparison between $Cu_3(dpa)_4Cl_2$ and the still hypothetical $Ag_3(dpa)_4Cl_2$. The question of electron delocalization along the metal chains will be discussed in both the neutral and the monooxidized species, in comparison with previous investigations and in relation to the results of the STM study of electron transfer.[16] The magnetic interactions, modeled

(7) (a) Tejel, C.; Ciriano, M. A.; López, J. A.; Lahoz, F. J.; Oro, L. A. *Angew. Chem., Int. Ed. Engl.* **1998**, *37*, 1542. (b) Tejel, C.; Ciriano, M. A. *Chem.—Eur. J.* **1999**, *5*, 1131. (c) Tejel, C.; Ciriano, M. A.; Villarroya, B. E.; Gelpi, R.; López, J. A.; Lahoz, F. J.; Oro, L. A. *Angew. Chem., Int. Ed.* **2001**, *40*, 4084. (d) Tejel, C.; Ciriano, M. A.; Villarroya, B. E.; López, J. A.; Lahoz, F. J.; Oro, L. A. *Angew. Chem., Int. Ed.* **2003**, *42*, 530. (e) Villarroya, B. E.; Tejel, C.; Rohmer, M.-M.; Oro, L. A.; Ciriano, M. A.; Bénard, M. **2005**, *44*, 6536.

(8) (a) Murahashi, T.; Kurosawa, H. *Coord. Chem. Rev.* **2002**, *231*, 207. (b) Murahashi, T.; Uemura, T.; Kurosawa, H. *J. Am. Chem. Soc.* **2003,** *125*, 8436. (c) Tatsumi, Y.; Naga, R.; Nakashima, H. Murahashi, T.; Kurosawa, H. *Chem. Commun.* **2004**, 1430.

(9) Wagaw, S.; Buchwald, S. L. *J. Org. Chem.* **1996**, *61*, 7240.

(10) Berry, J. F.; Cotton, F. A.; Lu, T.; Murillo, C. A. *Inorg. Chem.* **2003**, 42, 4425.

(11) Yang, E.-C.; Cheng, M.-C.; Tsai, M.-S.; Peng, S.-M. *J. Chem. Soc., Chem. Commun.* **1994**, *20*, 2377.

(12) (a) Cotton, F. A.; Daniels, L. M.; Jordan, T. J., IV. *Chem. Commun.* **1997**, 421. (b) Cotton, F. A.; Daniels, L. M.; Jordan, T. J., IV; Murillo, C. A. *J. Am. Chem. Soc.* **1997**, *119*, 10377. (c) Cotton, F. A.; Murillo, C. A.; Wang, X. *Inorg. Chem.* **1999**, *38*, 6294. (d) Cotton, F. A.; Murillo, C. A.; Wang, X. *J. Chem. Soc., Dalton Trans.* **1999**, 3327. (e) Clérac, R.; Cotton, F. A.; Dunbar, K. R.; Lu, T.; Murillo, C. A.; Wang, X. *J. Am. Chem. Soc.* **2000**, *122*, 2272. (f) Clérac, R.; Cotton, F. A.; Daniels, L. M.; Dunbar, K. R.; Kirschbaum, K.; Murillo, C. A.; Pinkerton, A. A.; Schultz, A. J.; Wang, X. *J. Am. Chem. Soc.* **2000**, *122*, 6226. (g) Clérac, R.; Cotton, F. A.; Dunbar, K. R.; Lu, T.; Murillo, C. A.; Wang, X. *Inorg. Chem.* **2000**, *39*, 3065. (h) Clérac, R.; Cotton, F. A.; Daniels, L. M.; Dunbar, K. R.; Murillo, C. A.; Wang, X. *J. Chem. Soc., Dalton Trans.* **2001**, 386. (i) Clérac, R.; Cotton, F. A.; Daniels, L. M.; Dunbar, K. R.; Murillo, C. A.; Wang, X. *Inorg. Chem.* **2001**, *40*, 1256. (j) Clérac, R.; Cotton, F. A.; Jeffery, S. P.; Murillo, C. A.; Wang, X. *Inorg. Chem.* **2001**, *40*, 1265.

(13) Sheng, T.; Appelt, R.; Comte, V.; Vahrenkamp, H. *Eur. J. Inorg. Chem.* **2003**, 3669.

(14) Berry, J. F.; Cotton, F. A.; Lu, T.; Murillo, C. A.; Roberts, B. K. *Inorg. Chem.* **2004**, *43*, 2277.

(15) (a) Cotton, F. A.; Daniels, L. M.; Murillo, C. A.; Pascual, I. *J. Am. Chem. Soc.* **1997**, *119*, 10223. (b) Cotton, F. A.; Daniels, L. M.; Murillo, C. A.; Pascual, I. *Inorg. Chem. Commun.* **1998**, *1*, 1. (c) Cotton, F. A.; Daniels, L. M.; Murillo, C. A.; Wang, L.-S. *Chem. Commun.* **1998**, 39. (d) Clérac, R.; Cotton, F. A.; Daniels, L. M.; Dunbar, K. R.; Murillo, C. A.; Pascual, I. *Inorg. Chem.* **2000**, *39*, 748. (e) Clérac, R.; Cotton, F. A.; Daniels, L. M.; Dunbar, K. R.; Murillo, C. A.; Pascual, I. *Inorg. Chem.* **2000**, *39*, 752. (f) Clérac, R.; Cotton, F. A.; Daniels, L. M.; Dunbar, K. R.; Murillo, C. A.; Zhou, H.-C. *Inorg. Chem.* **2000**, *39*, 3414. (g) Cotton, F. A.; Lei, P.; Murillo, C. A.; Wang, L.-S. *Inorg. Chim. Acta* **2003**, *349*, 165. (h) Cotton, F. A.; Lei, P.; Murillo, C. A. *Inorg. Chim. Acta* **2003**, *349*, 173. (i) Berry, J. F.; Cotton, F. A.; Lu, T.; Murillo, C. A.; Roberts, B. K.; Wang, X. *J. Am. Chem. Soc.* **2004**, *126*, 7082. (j) Li, H.; Lee, G.-H.; Peng, S.-M. *J. Mol. Struct.* **2004**, *707*, 179.

(16) Lin, S.-Y.; Chen, I. P.; Chen, C.-H.; Hsieh, M.-H.; Yeh, C.-Y.; Lin, T.-W.; Chen, Y.-H.; Peng, S.-M. *J. Phys. Chem. B* **2004**, *108*, 959.

(17) (a) Chang, H.-C.; Li, J.-T.; Wang, C.-C.; Lin, T.-W.; Lee, H.-C.; Lee, G.-H.; Peng, S.-M. *Eur. J. Inorg. Chem.* **1999**, 1243. (b) Shieh, S.-J.; Chou, C.-C.; Lee, G.-H.; Wang, C.-C.; Peng, S.-M. *Angew. Chem., Int. Ed. Engl.* **1997**, *36*, 56. (c) Wang, C.-C.; Lo, W.-C.; Chou, C.-C.; Lee, G.-H.; Chen, J.-M.; Peng, S.-M. *Inorg. Chem.* **1998**, *37*, 4059.

(18) (a) Rohmer, M.-M.; Bénard, M. *J. Am. Chem. Soc.* **1998**, *120*, 9372. (b) Rohmer, M.-M.; Strich, A.; Bénard, M.; Malrieu, J.-P. *J. Am. Chem. Soc.* **2001**, *123*, 9126.

(19) Benbellat, N.; Rohmer, M.-M.; Bénard, M. *Chem. Commun.* **2001**, 2368. Note that the structure of $Cr_3(dpa)_4Cl_2$ in the solid state is most certainly *unsymmetrical*, even though the DFT calculations carried out on the isolated molecule predict the structure with identical Cr−Cr bond lengths to be lowest in energy.

(20) Kiehl, P.; Rohmer, M.-M.; Bénard, M. *Inorg. Chem.* **2004**, *43*, 3151.

in the four systems by means of the broken-symmetry approach of Ginsberg[22] and Noodleman,[23−27] are interpreted in terms of two or three magnetic orbitals, depending on the molecular oxidation state. These magnetic orbitals are largely delocalized over the nitrogen ends of the equatorial ligands. Finally, the superexchange pathways of the antiferromagnetic interaction connecting the terminal copper atoms in $Cu_3(dpa)_4Cl_2$ and in $[Cu_3(dpa)_4Cl_2]^+$ have been characterized from an analysis of the response of the magnetic coupling constant, $2J$, to variations imposed on the Cu−Cu and to the Cu−N distances.

Computational Details

Calculations and geometry optimizations have been carried out with the Gaussian98 software,[28] using the formalism of the density functional theory (DFT), with the B3LYP exchange-correlation functional. Double-ζ valence basis sets have been used for all atoms, either including all electrons in the basis set for the first-row atoms (D95V bases) or describing the core of Cl and metal atoms with Los Alamos electron-core potentials (LanL2DZ bases). Atomic basis sets of similar quality have been shown to reproduce with sufficient accuracy the geometry and magnetic properties of $Ni_3(dpa)_4Cl_2$. The magnetic properties of this compound were also little affected by the inclusion of polarization functions.[20] All results discussed in the present work have therefore been obtained with the above-mentioned basis set. However, calibration calculations carried out on $Cu_3(dpa)_4Cl_2$ show that the basis set extension and the change or the removal of the core potential may have nonnegligible and opposite effects on computed J values.[21] The antiferromagnetic low-spin states of $M_3(dpa)_4Cl_2$ and $[M_3(dpa)_4Cl_2]^+$ (M = Cu, Ag) have been characterized, and their geometries have been optimized using the broken-symmetry (BS) formalism first proposed by Ginsberg,[22] standardized by Noodleman,[23] discussed and currently used by others.[24−27] The exchange parameter $2J_{AB}$ between two magnetic centers A and B is defined as follows by the Heisenberg−Dirac−van Vleck (HDVV) Hamiltonian[29]

$$\hat{H}^{HDVV} = -2J_{AB}\hat{S}_A\hat{S}_B \qquad (1)$$

whose eigenvalues are associated with the relative energies, $E^T = -2J_{AB}$ and $E^S = 0$ for $S_A = S_B = 1/2$.

It is clear that the nature of the ground state depends on the sign of J_{AB}: a positive value of J_{AB}, corresponding to a ferromagnetic interaction, designates the state with highest spin multiplicity as the ground state. Conversely, an antiferromagnetic interaction reverses the sign of J_{AB} and the energy ordering of the spin states. In either case, the BS solution lies between them, and its energy is equal to $E_{BS} = -J_{AB}$ if the overlap between the magnetic orbitals is neglected. It is also strongly spin-contaminated and displays a value of $<S^2>$ close to 1.0, as would be expected for a 50% admixture of singlet and triplet.[24e]

For a system involving three interacting magnetic centers A, B, and A′≡A, the HDVV Hamiltonian takes the following form

$$\hat{H} = -2J_{AB}(\hat{S}_A\hat{S}_B + \hat{S}_{A'}\hat{S}_B) - 2J_{AA'}\hat{S}_A\hat{S}_{A'} \qquad (2)$$

When all three magnetic centers correspond to $S = 1/2$, the eigenvalues are two doublet and one quartet states with following energies and spin distributions

$$E^Q(\uparrow\uparrow\uparrow) = -3J_{AB} \qquad E^{D1}(\uparrow\uparrow\downarrow) = -2J_{AB} + 2J_{AA'} \qquad E^{D2}(\uparrow\downarrow\uparrow) = 0 \qquad (3)$$

Since the doublet state D1 of intermediate energy does not affect, in practice, the measured magnetic properties, the $J_{AA'}$ exchange parameter is not relevant and can be overlooked.

At this point, a controversy has developed concerning the interpretation of the energy associated with the BS solution and

(21) The magnetic coupling constant for $Cu_3(dpa)_4Cl_2$ was calculated to be $-2J = 436.5\ cm^{-1}$ with the LanL2DZ bases (Table 3). Inclusion of *diffuse* functions on all non-H atoms hardly modified this value to $426.8\ cm^{-1}$. A plain augmentation of the LanL2DZ basis sets with f-type polarization functions on copper (ζ = 3.525) and d-type polarization functions on N (ζ = 0.80) and Cl (ζ = 0.64) atoms yielded an *increase* of $-2J = 497.1\ cm^{-1}$. However, the use of an all-electron 6-311G* basis for Cl, N, C, H and of a triple-ζ basis for the valence shell of Cu augmented with one f-type polarization function (ζ = 3.525), completed with the quasirelativistic Stuttgart-Dresden effective core potential describing the Ne core (Andrae, D.; Haüssermann, U.; Dolg, M.; Stoll, H.; Preuss, H. *Theor. Chim. Acta*, **1990**, *77*, 123), yielded a value of $-2J = 329.3\ cm^{-1}$.

(22) Ginsberg, A. P. *J. Am. Chem. Soc.* **1980**, *102*, 111.
(23) (a) Noodleman, L. *J. Chem. Phys.* **1981**, *74*, 5737. (b) Noodleman, L.; Baerends, E. J. *J. Am. Chem. Soc.* **1984**, *106*, 2316. (c) Noodleman, L.; Davidson, E. R. *Chem. Phys.* **1986**, *109*, 131. (d) Noodleman, L.; Norman, J. G., Jr.; Osborne, J. H.; Aizman, A.; Case, D. A. *J. Am. Chem. Soc.* **1985**, *107*, 3418. (f) Noodleman, L.; Case, D. A.; Aizman, A. *J. Am. Chem. Soc.* **1988**, *110*, 1001. (g) Noodleman, L.; Peng, C. Y.; Case, D. A.; Mouesca, J. M. *Coord. Chem. Rev.* **1995**, *144*, 199.
(24) (a) Caballol, R.; Castell, O.; Illas, F.; Malrieu, J.-P.; de P. R. Moreira, I. *J. Phys. Chem. A* **1997**, *101*, 7860. (b) Martin, R. L.; Illas, F. *Phys. Rev. Lett.* **1997**, *79*, 1539. (c) Illas, F.; Martin, R. L. *J. Chem. Phys.* **1998**, *108*, 2519. (d) Cabrero, J.; Calzado, C. J.; Maynau, D.; Caballol, R.; Malrieu, J.-P. *J. Phys. Chem. A* **2002**, *106*, 8146. (e) Illas, F.; de P. R. Moreira, I.; de Graaf, C.; Barone, V. *Theor. Chem. Acc.* **2000**, *104*, 265.
(25) (a) Yamaguchi, K.; Fukui, H.; Fueno, T. *Chem. Lett.* **1986**, 625. (b) Yamaguchi, K.; Takahara, Y.; Fueno, T.; Nasu, K. *Japan. J. Appl. Phys.* **1987**, *26*, L1362. (c) Mitani, M.; Mori, H.; Takano, Y.; Yamaki, D.; Yoshioka, Y.; Yamaguchi, K. *J. Chem. Phys.* **2000**, *113*, 4035. (d) Onishi, T.; Soda, T.; Kitagawa, Y.; Takano, Y.; Daisuke, Y.; Takamizawa, S.; Yoshioka, Y.; Yamaguchi, K. *Mol. Cryst. Liq. Cryst.* **2000**, *143*, 133. (e) Onishi, T.; Takano, Y.; Kitagawa, Y.; Kawakami, T.; Yoshioka, Y.; Yamaguchi, K. *Polyhedron* **2001**, *20*, 1177.
(26) (a) Petrie, S.; Stranger, R. *Inorg. Chem.* **2002**, *41*, 2341. (b) Stranger, R.; Petrie, S. *J. Chem. Soc., Dalton Trans.* **2002**, 1163. (c) Petrie, S.; Stranger, R. *Polyhedron* **2002**, *21*, 1163 and references therein. (d) Delfs, C. D.; Stranger, R. *Inorg. Chem.* **2001**, *40*, 3061. (e) Duclusaud, H.; Borshch, S. A. *J. Am. Chem. Soc.* **2001**, *123*, 2825. (f) Blasco, S.; Demachy, I.; Jean, Y.; Lledós, A. *New J. Chem.* **2002**, *26*, 1118. (g) Blasco, S.; Demachy, I.; Jean, Y.; Lledós, A. *Inorg. Chim. Acta* **2000**, *300−302*, 837. (h) Demachy, I.; Lledós, A.; Jean, Y. *Inorg. Chem.* **1999**, *38*, 5443. (i) Demachy, I.; Jean, Y.; Lledós, A. *Chem. Phys. Lett.* **1999**, *303*, 621. (j) Lledós, A.; Jean, Y. *Chem. Phys. Lett.* **1998**, *287*, 243.
(27) (a) Ruiz, E.; Alvarez, S.; Cano, J.; Polo, V. *J. Chem. Phys.* **2005**, *123*, 64110. (b) Ruiz, E. *Struct. Bond.* **2004**, *113*, 71. (c) Ruiz, E.; Alvarez, S.; Rodríguez-Fortea, A.; Alemany, P.; Pouillon, Y.; Massobrio, C. In *Magnetism: Molecules to Materials*; Miller, J. S., Drillon, M., Eds.; Wiley-VCH: Weinheim, Germany, 2001; Vol. 2, p 227. (d) Ruiz, E.; Alemany, P.; Alvarez, S.; Cano, J. *J. Am. Chem. Soc.* **1997**, *119*, 1297.
(28) Frisch, M. J.; Trucks, G. W.; Schlegel, H. B.; Scuseria, G. E.; Robb, M. A.; Cheeseman, J. R.; Zakrzewski, V. G.; Montgomery, J. A., Jr.; Stratmann, R. E.; Burant, J. C.; Dapprich, S.; Millam, J. M.; Daniels, A. D.; Kudin, K. N.; Strain, M. C.; Farkas, O.; Tomasi, J.; Barone, V.; Cossi, M.; Cammi, R.; Mennucci, B.; Pomelli, C.; Adamo, C.; Clifford, S.; Ochterski, J.; Petersson, G. A.; Ayala, P. Y.; Cui, Q.; Morokuma, K.; Malick, D. K.; Rabuck, A. D.; Raghavachari, K.; Foresman, J. B.; Cioslowski, J.; Ortiz, J. V.; Stefanov, B. B.; Liu, G.; Liashenko, A.; Piskorz, P.; Komaromi, I.; Gomperts, R.; Martin, R. L.; Fox, D. J.; Keith, T.; Al-Laham, M. A.; Peng, C. Y.; Nanayakkara, A. Gonzalez, C.; Challacombe, M.; Gill, P. M. W.; Johnson, B. G.; Chen, W.; Wong, M. W.; Andres, J. L.; Head-Gordon, M.; Replogle, E. S.; Pople, J. A. *Gaussian 98*, revision A.6; Gaussian, Inc.: Pittsburgh, PA 1998.
(29) (a) Dirac, P. A. M. *Proc. R. Soc. London, Ser. A* **1926**, *112*, 661; **1929**, *123*, 714. (b) Heisenberg, W. *Z. Phys.* **1926**, *38*, 411. (c) van Vleck, J. H. *Theory of Electric and Magnetic Susceptibilities*; Oxford University Press: London, 1932. (d) Kahn, O. *Molecular Magnetism;* Wiley-VCH: New York, 1993.

the way to use it within the DFT/B3LYP framework. While some authors maintain that the real ground-state energy should be deduced from the BS solution via a convenient spin projection, as in the ab initio UHF framework, Ruiz and co-workers advocate the use of the nonprojected BS energy as the best approximation to the real ground-state energy.[27] The discrepancy between these approaches is maximal in the case of a two-electron problem, for which it amounts a factor of 2.[27] For the three-electron case developed above, the single-determinant broken-symmetry solution computed according to Noodleman's formalism should correspond, *if the overlap between the magnetic orbitals is strictly zero*, to an energy of $E^{BS} = -J_{AB}$, closer in this case to the energy of the real antiferromagnetic D2 state. To deal with real cases, Yamaguchi et al proposed an elegant spin projection procedure, valid for 2 and 3 magnetic centers[25] in which the dependence of $2J_{ab}$ upon the overlap is replaced by a dependence upon the spin contamination of the broken symmetry solution

$$2J_{ab} = 2({}^{BS}E - {}^{HS}E)/({}^{HS}\langle S^2\rangle - {}^{BS}\langle S^2\rangle) \qquad (4)$$

where ${}^{HS}\langle S^2\rangle$ and ${}^{BS}\langle S^2\rangle$ denote the total spin angular momentum calculated in the high-spin and broken-symmetry solutions, respectively. ${}^{BS}\langle S^2\rangle$ can in principle vary from the eigenvalue of the real low-spin state to a maximal value ${}^{BS}\langle S^2\rangle_{max}$ corresponding to the weighted admixture of the states with higher multiplicity. A computed value of ${}^{BS}\langle S^2\rangle$ close to ${}^{BS}\langle S^2\rangle_{max}$ indicates a negligible overlap between magnetic orbitals.[25] In this case with three identical magnetic centers of $S = 1/2$, ${}^{BS}\langle S^2\rangle_{max}$ is equal to 1.75. For the sake of consistency with the previous work carried out on linear triatomics, Yamaguchi's projection has been used in the present study, even though results closer to those of the experiment should be deduced from a nonprojected formalism.

All geometry optimizations have been carried out assuming the symmetry constraints of either the D_4 or, for the broken-symmetry calculations, of the C_4 symmetry point groups.

$M_3(dpa)_4Cl_2$ Complexes: Orbital Occupancies and Interactions along the Metal Chain

The 15 molecular orbitals (MOs) with dominant metal character generated in $M_3(dpa)_4L_2$ complexes with D_4 symmetry and their energy sequence have been discussed previously.[18−20] They are schematized in Figure 2. At both ends of the complex, the presence of σ-donor ligands in axial positions raises the energy of the σ MOs and modifies the coordination field from square planar to square pyramidal, which tends to promote a high-spin configuration in metals such as Co^{II} or Ni^{II}. The occupancy scheme of the metal MOs in the ground state of $M_3(dpa)_4L_2$ complexes will therefore depend on the interplay between the number of electrons to be accommodated, the rigidity of the dpa coating, the donor strength of the axial ligands, and the tendency of the metal chain to generate delocalized bonds. These occupancies are schematized in Figure 3 for M = Cr, Co, Ni, and Cu.

Apart from $Co_3(dpa)_4Cl_2$, whose doublet ground state is in accordance with the Aufbau principle, none of the trimetallic species can be properly described according to the sole sequence of orbital energies. As far as $Cu_3(dpa)_4Cl_2$ is concerned, the magnetic studies have shown that the ground state has one unpaired electron and is separated by

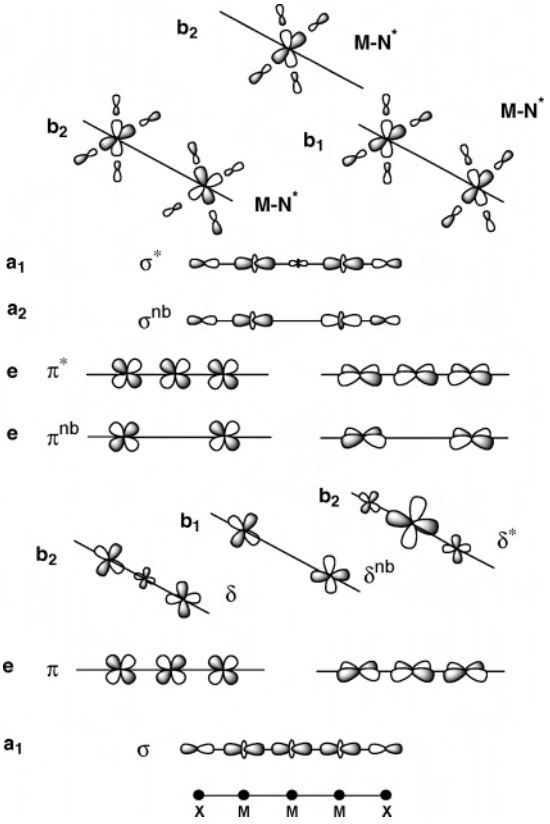

Figure 2. Sequence of metal molecular orbitals obtained for $M_3(dpa)_4Cl_2$.

560 cm^{-1} from a higher quartet state.[30,31] This situation could be interpreted in terms of either (i) a localized picture in which three nonbonded Cu(II) ions are spin-coupled to give a doublet or a quartet state or (ii) a delocalized model based on a three-electron/three-center bond involving 4s orbital combinations.[15i] Experimental information was said to be indecisive with respect to that dilemma. A comparison between the observed structures of neutral $Cu_3(dpa)_4L_2$ (L = Cl, **1**; BF_4, **2**)[4,31] and that of the oxidized species $[Cu_3(dpa)_4Cl_2]SbCl_6$ (**3**)[30] however provides some clues (Table 1). On one hand, the $Cu-N_{outer}$ bond lengths in **1**, **2**, and **3** are all in the range of 2.05−2.09 Å and compare well with the $Ni-N_{outer}$ distances observed for $Ni_3(dpa)_4L_2$ complexes (2.08−2.10 Å).[32] In this family of complexes, the $Ni-N_{outer}$ distances are elongated because of the half-occupancy of the two high-energy δ MOs with $Ni-N_{outer}$ antibonding character. When these orbitals are vacant, as in $[Ni_3(BPAP)_4]^{2-}$, the Ni−N bond lengths are much shorter (1.90−1.92 Å).[32b] On the other hand, the $M-N_{inner}$ bond lengths in the neutral copper species **1** and **2** are longer by 0.07−0.09 Å than in the equivalent compounds of nickel,

(30) Berry, J. F.; Cotton, F. A.; Daniels, L. M.; Murillo, C. A.; Wang, X. *Inorg. Chem.* **2003**, *42*, 2418.
(31) Berry, J. F.; Cotton, F. A.; Lei, P.; Murillo, C. A. *Inorg. Chem.* **2003**, *42*, 377.
(32) (a) Clérac, R.; Cotton, F. A.; Dunbar, K. R.; Murillo, C. A.; Pascual, I.; Wang, X. *Inorg. Chem.* **1999**, *38*, 2655. (b) Cotton, F. A.; Daniels, L. M.; Lei, P.; Murillo, C. A.; Wang, L.-S. *Inorg. Chem.* **2001**, *40*, 2778. (c) Berry, J. F.; Cotton, F. A.; Lu, T.; Murillo, C. A.; Wang, X. *Inorg. Chem.* **2003**, *42*, 3595. (d) Cotton, F. A.; Lei, P.; Murillo, C. A. *Inorg. Chim. Acta* **2003**, *351*, 183. (e) Berry, J. F.; Cotton, F. A.; Murillo, C. A. *Dalton Trans.* **2003**, 3015.

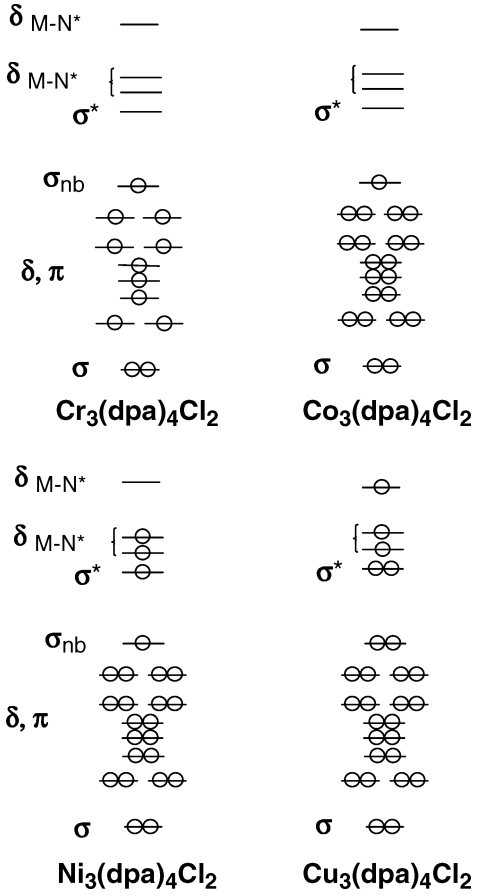

Figure 3. Metal orbital occupancies in $M_3(dpa)_4Cl_2$ complexes, not accounting for the possibility of spin couplings between the unpaired electrons.

Table 1. Selected Distances (Å) Observed for $Cu_3(dpa)_4Cl_2$ (**1**), $Cu_3(dpa)_4(BF_4)_2$ (**2**), and $[Cu_3(dpa)_4Cl_2]SbCl_6$ (**3**)

	1[a]	**2**	**3**[a]
Cu−Cu	2.467−2.492	2.403	2.505−2.513
Cu−L	2.436−2.487	2.239−2.254	2.388−2.392
$Cu-N_{outer}$	2.061−2.088	2.049	2.061−2.065
$Cu-N_{inner}$	1.958−1.983	1.972	1.885−1.886
ref	31	31	30

[a] Lowest and highest values obtained from measurements carried out with crystals including different interstitial solvent molecules and at different temperatures.[31]

but oxidation of **1** into **3** reduces the $Cu-N_{inner}$ bond lengths by a similar amount. Such a contraction of the central bonds is *not* observed in $[Ni_3(dpa)_4Cl_2]^+$.[32c]

It can be suggested from these observations that (i) all three high-lying δ MOs exhibiting antibonding Cu−N character are singly occupied in the ground state of **1** and **2**, as shown in Figure 3 and that (ii) the oxidation process removes an electron from the orbital indeed highest in energy, which displays its major weight on the central metal and on its equatorial environment. This implies that combinations of the copper 4s orbitals do not directly take part in the ground state of either the neutral or the oxidized species. The $Cu_3(dpa)_4Cl_2$ compounds are therefore expected to conform to a localized picture in which three electrons distributed each on a metal atom and its equatorial environment are spin-coupled according to the top part of Figure 4.

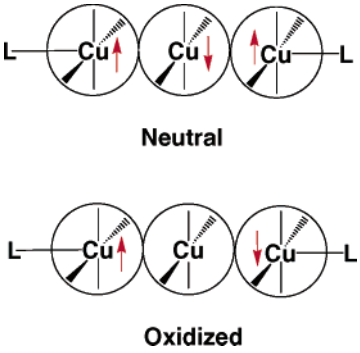

Figure 4. Scheme of the antiferromagnetic couplings proposed for $Cu_3(dpa)_4L_2$ (L = Cl, BF_4) and $[Cu_3(dpa)_4Cl_2]^+$.

The removal of one electron from the inner metal upon oxidation yields an antiferromagnetic coupling between the outer $Cu-N_4$ moieties (Figure 4, bottom). These assumptions have been confirmed by the DFT calculations, as will be discussed in the next section.

Finally, the formal strength of the M−M−M bonding in $M_3(dpa)_4Cl_2$ should be deduced from the orbital occupancies of Figure 3. Both $Cr_3(dpa)_4Cl_2$ and $Co_3(dpa)_4Cl_2$ in their symmetric forms display similar 3-electron/3-center σ bonds characterized by the full occupancy of the σ-bonding MO and the half-occupancy of the nonbonding σ combination. On the top of this σ bond, the chromium complex displays an attractive interaction involving the nine electrons accommodated in the π and δ orbitals, which could be interpreted either as a strong antiferromagnetic exchange between the inner and the outer metal atoms or as a weak multiple bonding delocalized along the trimetallic framework. This type of multiple bonding is specific to the symmetric $Cr_3(dpa)_4L_2$ and $Ru_3(dpa)_4L_2$[33] complexes, since in other $M_3(dpa)_4Cl_2$ species, all π and low-energy δ levels are doubly occupied and do not take part in the bonding. $Ni_3(dpa)_4Cl_2$ still displays some delocalized interaction in relation with the single occupancy of the antibonding σ MO. The complexes of copper and silver are the only ones of this series for which no formal bonding between metal atoms can be associated with their electronic configuration. It therefore appears that the formal strength of the delocalized bonding in symmetric $M_3(dpa)_4Cl_2$ compounds follows the order

$$Cr > Co > Ni > Cu \qquad (5)$$

It is interesting that the ordering, Cr > Co > Ni, correlates with the relative ability of the corresponding $M_3(dpa)_4(NCS)_2$ species to transfer electrons along the metal framework, as deduced from STM experiments.[16] The discrepancies observed in the STM results as a function of the nature of the metal have been attributed to electron localization−delocalization among the metal centers.[16] The present analysis confirms this correlation and suggests that $M_3(dpa)_4L_2$ complexes made with coinage metal frameworks should provide the lowest response to STM stimulation.

$M_3(dpa)_4Cl_2$ and $[M_3(dpa)_4Cl_2]^+$(M = Cu, Ag): Computed Structure And Magnetic Interactions

The main geometrical parameters optimized for the neutral and oxidized forms of $Cu_3(dpa)_4Cl_2$ and $Ag_3(dpa)_4Cl_2$ are

Table 2. Selected Distances (Å) and Angles (deg) Computed for $Cu_3(dpa)_4Cl_2$, $[Cu_3(dpa)_4Cl_2]^+$, $Ag_3(dpa)_4Cl_2$, $[Ag_3(dpa)_4Cl_2]^+$, and $Cu_3(dpa)_4(BF_4)_2$ in Their Low-Spin Ground States, Approximated by the Broken-Symmetry Solution

	$Cu_3(dpa)_4Cl_2$	$[Cu_3(dpa)_4Cl_2]^+$	$Ag_3(dpa)_4Cl_2$	$[Ag_3(dpa)_4Cl_2]^+$	$Cu_3(dpa)_4(BF_4)_2$
M−M	2.525	2.571	2.675	2.695	2.444
M−L	2.535	2.470	2.672	2.627	2.181
$M-N_{outer}$	2.097	2.084	2.296	2.266	2.064
$M-N_{inner}$	1.999	1.922	2.186	2.093	2.006
$N-M_{outer}-N$	163.5	161.0	159.9	158.9	168.7

Table 3. Atomic Spin Populations ($\alpha-\beta$, electrons), Values of $<S^2>$, High-Spin (HS)−Broken-Symmetry (BS) Energy Differences, ΔE (kcal mol^{-1}), and Exchange Parameters, $-2J$ (cm^{-1}), Computed for $Cu_3(dpa)_4Cl_2$, $[Cu_3(dpa)_4Cl_2]^+$, $Ag_3(dpa)_4Cl_2$, and $[Ag_3(dpa)_4Cl_2]^+$[a]

	$Cu_3(dpa)_4Cl_2$		$[Cu_3(dpa)_4Cl_2]^+$		$Ag_3(dpa)_4Cl_2$		$[Ag_3(dpa)_4Cl_2]^+$	
$\alpha-\beta$	HS	BS	HS	BS	HS	BS	HS	BS
M_{outer}	0.58	0.59	0.59	±0.59	0.38	0.35	0.38	±0.38
M_{inner}	0.52	−0.54	0.045	0.0	0.35	−0.31	0.031	0.0
Cl	0.00	0.00	0.00	0.00	0.00	0.00	0.00	0.00
N_{outer}	0.11	0.10	0.10	±0.10	0.16	0.14	0.15	±0.15
N_{inner}	0.11	−0.10	0.001	0.0	0.15	−0.12	0.010	0.0
$<S^2>$	3.76	1.72	2.01	1.02	3.76	1.49	2.01	1.01
ΔE	+1.24	0.0	+0.09	0.0	+4.12	0.0	+0.38	0.0
$-2J$[b]	436.5 *(372.6)*		64 *(34)*		1270		265	

[a] Energies and spin densities for the high-spin states are calculated assuming the optimal geometry of the BS state. Full optimization of the high spin state produces no significant change, except for the magnetic exchange parameter of $Ag_3(dpa)_4Cl_2$, which is reduced by ∼10%. [b] Experimental values in parentheses.

displayed in Table 2. All distances are slightly overestimated by 0.03−0.07 Å, but the structural trends entailed by ionization are nicely reproduced. Ionization of $Cu_3(dpa)_4Cl_2$ induces an expansion of the metal−metal distances and a contraction of the Cu−Cl bond lengths that can be assigned to the increased positive charge on the metal atoms (Tables 1 and 2).

The replacement of Cl by BF_4 in the axial position contracts the Cu−Cu distance by 0.08 Å, in agreement with the X-ray structures (Tables 1 and 2). Since $(BF_4)^-$ is a weaker σ-donor than Cl^-, the contraction of the Cu····Cu distance should be correlated to this decrease of the axial ligand field, which tends to modify the coordination field from square-pyramidal to square planar. The contraction of the Cu····Cu distance accounts for this trend, as the $N-Cu_{outer}-N$ angle opens from 163.5° to 168.7° (Table 2). Other geometrical changes, such as the contraction (0.03 Å) of the $Cu_{outer}-N$ distances with respect to $Cu_3(dpa)_4Cl_2$, are in agreement with this interpretation and with the X-ray data (Tables 1 and 2).

Antiferromagnetic interactions in neutral $Cu_3(dpa)_4Cl_2$ involve the density associated with three electrons originating each on a definite metal center, but spreading through the high energy δ MOs over its equatorial nitrogen environment (Figure 4). The atomic spin densities calculated for the BS state confirm this expansion of the magnetic orbitals. The spin densities are +0.59 e and −0.54 e on the outer and inner metal atoms, respectively, whereas the nitrogens provide the remaining ∼40% of the spin density (Table 3). The magnetic exchange parameter calculated from projection formula 4 is $-2J = 436.5\ cm^{-1}$, in reasonable agreement with the value of $-372.6\ cm^{-1}$ deduced from magnetic susceptibility measurements. However, it should be kept in mind that the computed values of $-2J$ are extremely sensitive to the technical parameters of the calculation.[21,24,27] Determination of the magnetic exchange pathways represents an interesting problem. On one hand, experimental investigation on $Cu_3(dpa)_4(BF_4)_2$ shows that $-2J$ increases by 38 cm^{-1} with respect to $Cu_3(dpa)_4Cl_2$, whereas the metal−metal distance contracts by ∼0.07 Å, suggesting that a direct exchange mechanism, such as a metal−metal interaction, might contribute to the antiferromagnetic coupling.[31] On the other hand, the three magnetic orbitals in $Cu_3(dpa)_4L_2$ are x^2-y^2-like orbitals oriented toward the four nitrogen atoms of the equatorial ligand environment, a situation reminiscent of the carboxylato-bridged dinuclear copper(II) complexes for which a Cu···Cu "superexchange" coupling has been shown to occur via the bridging ligands.[34,35] To solve this dilemma, we have considered a hypothetic $Cu_3(dpa)_4Cl_2$ complex in which the Cu−Cu distances have been contracted by 0.10 Å with respect to the optimal value of 2.525 Å. All Cu−N distances have been kept frozen to their optimal values and the other geometrical parameters have been reoptimized for the BS state. The value of $-2J$ calculated for this complex with closer metal−metal contacts is 428.4 cm^{-1}.[36] Even though the difference of 8 cm^{-1} between the two calculations is weak, a *decrease* of $-2J$ with the metal−metal distance strongly suggests that the coupling occurs via the bridging ligands.[37] We therefore propose an extension to three centers of the ligand exchange coupling documented by Rodríguez-Fortea et al.[34] and others.[35] The corresponding pathways are represented in Figure 5.

Another important issue related to the magnetic exchange pathways in $Cu_3(dpa)_4L_2$ complexes resides in the interpretation of the observed 10% increase of $-2J$ when Cl ligands are replaced by BF_4. Unfortunately, the present calculations remain inconclusive on that point. Even though the geometrical changes associated with the weakening of σ donation are correctly reproduced (Tables 1, 2), the computed value

(33) Sheu, J.-T.; Lin, C.-C.; Chao, I.; Wang, C.-C.; Peng, S.-M. *Chem. Commun.* **1996**, 315.
(34) Rodríguez-Fortea, A.; Alemany, P.; Alvarez, S.; Ruiz, E. *Chem.—Eur. J.* **2001**, *7*, 627.
(35) (a) Goodgame, D. M. L.; Hill, N. J.; Marsham, D. F.; Scapoki, A. C.; Smart, M. L.; Throughton, P. G. H. *J. Chem. Soc., Chem. Commun.* **1969**, 629. (b) Jotham, R. W.; Kettle, S. F. A. *Inorg. Chem.* **1970**, *9*, 1390. (c) de Loth, P.; Cassoux, P.; Daudey, J. P.; Malrieu, J. P. *J. Am. Chem. Soc.* **1981**, *103*, 4007.
(36) Note that the relative energy computed for $Cu_3(dpa)_4Cl_2$ with Cu−Cu bond lengths contracted by 0.10 Å is no more than +1.9 kcal mol^{-1}, despite the constraints imposed to the Cu−N bond lengths.
(37) A similar enhancement of the antiferromagnetic coupling was computed in carboxylato-bridged dinuclear Cu(II) compounds when the Cu−Cu distance increases, an effect that can only be explained in terms of a superexchange mechanism via the carboxylate ligands.[34]

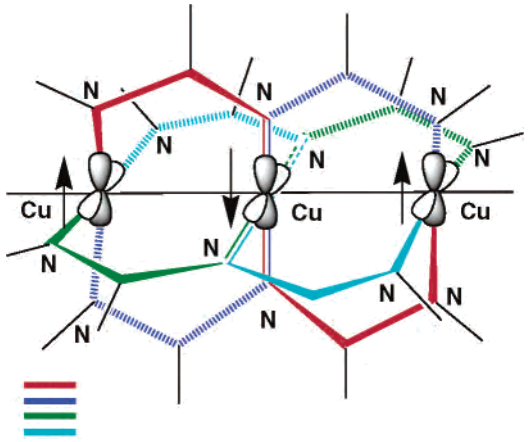

Figure 5. Pathways of the superexchange in $Cu_3(dpa)_4Cl_2$.

of $-2J$ does not display the expected increase but instead shows a 5% *decrease* at 415.7 cm^{-1}. This result only confirms that the significant contraction of the metal−metal distance is not correlated with the observed enhancement of the magnetic coupling. The other geometrical variations, and more specifically, the slight contraction of the Cu_{outer}−N distances, do not appreciably modify the spin distribution and the spin overlap populations along the metal−ligand pathway. Consequently, the observed variation of the magnetic coupling in $(Cu_3)^{6+}$ complexes cannot be presently assigned a definite origin.

In contrast with the change in axial coordination, the hypothetic replacement of copper by silver in $M_3(dpa)_4Cl_2$ induces a tremendous increase of the computed antiferromagnetic coupling, which increases from 436 to 1270 cm^{-1}. The electronic configuration of the complex and the nature of the magnetic orbitals remain similar to those of $Cu_3(dpa)_4Cl_2$ and exclude any rationalization based on the presence of a metal−metal bonding interaction. However, a clue is provided by the amount of spin contamination associated with the BS solution. For $Cu_3(dpa)_4Cl_2$, $^{BS}\langle S^2\rangle$ is computed to be 1.72, rather close to the maximal value of 1.75 corresponding to the case of three nonoverlapping magnetic orbitals. For $Ag_3(dpa)_4Cl_2$, $^{BS}\langle S^2\rangle$ decreases to 1.49, thus providing the first characterized example of a significant overlap between magnetic orbitals in a $M_3(dpa)_4L_2$ system. What is the origin of this overlap? Some direct overlap between the Ag−N antibonding δ orbitals of adjacent metals cannot be excluded, at variance with copper, in relation with the more diffuse valence d shell of second-row transition metals. This overlap is likely to remain weak, however, and most of the coupling should be again interpreted in terms of a superexchange mechanism involving the dpa ligands. One should therefore consider an increased overlap via the bridging ligands, in relation with a more balanced distribution of the spin density between the metal and surrounding nitrogens. Indeed, the replacement of Cu(II) by Ag(II) dramatically increases the negative spin overlap population between the metal and the equatorial ligands from −0.032 to −0.045 e along the outer M−N bonds and from −0.034 to −0.047 e along the inner bonds. The spin population on all nitrogen atoms also increases (Table 3). In the task of

Table 4. Variation of the Exchange Coupling Parameter $-2J$ (cm^{-1}) as a Function of the Cu−Cu and Cu−N Distances (Å), Values of the Total Atomic Spin Population, and Atomic Spin Density ($\alpha-\beta$, electrons) Associated with $d_{x^2-y^2}$ in the High-Spin State ($^3A_1$) for $[Cu_3(dpa)_4Cl_2]^+$

constrained distances		$-2J$	$\alpha-\beta$ Cu_{inner} (total)	$\alpha-\beta$ Cu_{inner} (x^2-y^2)
d_{Cu-Cu} (0)[a]	d_{Cu-N} (0)[a]	64	0.0448	0.061
d_{Cu-Cu} (+0.10)	d_{Cu-N} (0)	56	0.0427	0.056
d_{Cu-Cu} (−0.10)	d_{Cu-N} (0)	76	0.0500	0.069
d_{Cu-Cu} (0)	d_{Cu-N} (−0.05)	44	0.0314	0.049

[a] Optimal Cu−Cu distance is 2.571 Å; optimal Cu−N distances are as follows: $Cu-N_{outer}$ = 2.084 Å, $Cu-N_{inner}$ = 1.922 Å.

delineating the various effects influencing the exchange coupling constant in the Cu(II) carboxylates, the metal−oxygen overlap spin population can be considered as a comprehensive indicator, according to the analysis carried out by Rodríguez-Fortea et al.: accounting for the metal−ligand antibonding character of the SOMO, the more negative the Cu−O overlap spin population, the more negative (i.e., antiferromagnetic) is the coupling constant.[34] The linear correlation deduced from a series of calculations on various $L_2Cu_2(\mu\text{-}RCOO)_4$ complexes shows that a 3% variation of the overlap population associated with the magnetic orbitals changes the value of J by a factor of 4.[34] As a result of a stronger metal−ligand antibonding interaction, the Ag−N overlap spin populations become 40% more negative than their Cu−N homologues in the trinuclear complexes, which can explain the surge of the antiferromagnetic coupling constants.

Oxidation of $Cu_3(dpa)_4Cl_2$ removes one electron from the $Cu-N_{inner}$ antibonding orbital. It is interesting to notice that the positive charge does not remain localized on the inner $Cu-N_4$ moiety but is fully delocalized throughout the ligand envelope. The antiferromagnetic exchange parameter $-2J$ computed for the cation is 64 cm^{-1}, seven times weaker than that for the neutral complex, but still overestimated by a factor of 2 with respect to the experimental value of 34 cm^{-1} (Table 3).[38] In agreement with the scheme involving a coupling between two magnetic orbitals distributed over the $(Cu-N_4)_{outer}$ fragments (Figure 4, bottom) the central plane containing the $Cu-N_{inner}$ bonds becomes a plane of antisymmetry for the spin distribution in the BS state. However, an analysis of the spin distribution in the *high-spin state*, $^3A_1$, shows that the tail of the magnetic orbitals extends to Cu_{inner} and provides the central copper with some spin density (Table 4). The spin population of Cu_{inner} in the $^3A_1$ state of the cation is about 7% of its value in the neutral complex, which is sufficient for this atom to play a key role in the superexchange mechanism. As for the neutral complex, the pathways of the magnetic exchange have been investigated by separately constraining the Cu−Cu and the Cu−N bond lengths to deviate from their computed equilibrium values (Table 4). At variance with neutral $Cu_3(dpa)_4Cl_2$, the antiferromagnetic coupling becomes stronger when the Cu−Cu distance contracts, which could be a priori interpreted in favor of a direct coupling via the central copper atom. The coupling

(38) Note that the overestimation obtained for the cationic, as for the neutral, copper complexes would cancel by just using the unprojected formalism advocated by Ruiz et al.[27]

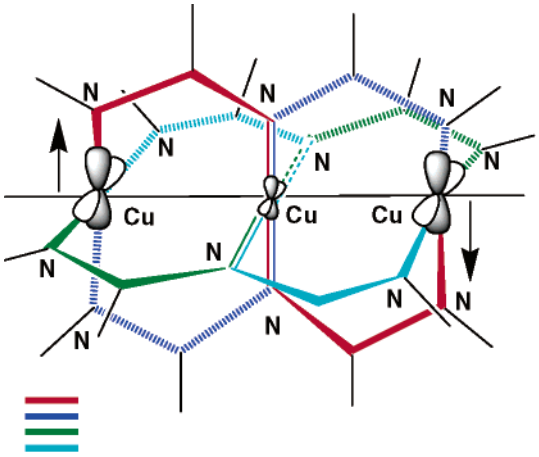

Figure 6. Pathways of the superexchange in $[Cu_3(dpa)_4Cl_2]^+$.

is also sensitive, however, to a concerted decrease of the twelve Cu−N bond lengths, and quite surprisingly, such a decrease *weakens* the antiferromagnetic coupling. These results could however be correlated with the variations of the spin population of Cu_{inner}, and, still more convincingly, with the changes of the spin population associated with the $d_{x^2-y^2}$ orbital of the same atom. Indeed, any strengthening of the antiferromagnetic coupling should be associated with an increase of the spin population along the $(Cu-N)_{inner}$ bonds (Table 4). The role of the spin polarization along the metal−ligand directions suggests that the x^2-y^2 orbital of the inner metal still lies at the crossing point of the magnetic interaction pathways, even though $(Cu-N_4)_{inner}$ is not an active magnetic center anymore (Figure 6).

Oxidation of the hypothetical $Ag_3(dpa)_4Cl_2$ modifies the nature and strength of the antiferromagnetic coupling in a manner similar to that for its copper homolog. The constant $-2J$ calculated for $[Ag_3(dpa)_4Cl_2]^+$ is 265 cm^{-1}, four times larger than for the tricopper cationic species (Table 3). For the triplet state, the spin polarization of the $(x^2-y^2)_{inner}$ orbital is 0.031 e, which is lower than for $[Cu_3(dpa)_4Cl_2]^+$. However, as for the outer metals, the spin polarization is now largely delocalized on the surrounding nitrogens (0.040 e on the four N atoms altogether, compared to 0.004 e for the copper cation, Table 3). The increase of the antiferromagnetic coupling in the Ag compound should therefore be attributed to a better overlap between the metal and equatorial ligands (i) in the magnetic orbitals of the $(Ag-N_4)_{outer}$ moieties and (ii) in the spin-polarized x^2-y^2 orbital of the inner metal, located at the meeting point of the superexchange pathways (Figure 6).

It is finally tempting to parallel the spin coupling in $[Cu_3(dpa)_4Cl_2]^+$ with that observed and computed in $Ni_3(dpa)_4Cl_2$. In the latter case, the antiferromagnetic coupling involves two electron pairs, both localized on the outer nickel atoms and their coordination environment.[32,20] One of these pairs is accommodated in the $d_{x^2-y^2}$-like orbitals of the outer metal atoms and generates a coupling via the dpa ligands resembling that of $[Cu_3(dpa)_4Cl_2]^+$. The other electron pair is described by two spin-polarized σ orbitals, each centered on one external Ni atom but providing some delocalization through the central nickel. It is therefore appealing to assign to this d_{z^2} pathway the magnified coupling observed in $Ni_3(dpa)_4Cl_2$ ($-2J_{obs}$ = 216 cm^{-1}).[32] This provides an opportunity to remember that the description of the magnetic coupling by means of the Heisenberg Hamiltonian is purely phenomenological. The interpretation through an unique constant of two couplings which appear quite different, even though originating in the same magnetic centers, is practical but not really physical. One should therefore refrain from considering that the J constants associated with different couplings should be additive, even approximately.

Summary and Conclusion

$Cu^{II}\cdots Cu^{II}$ distances in $Cu_3(dpa)_4L_2$ complexes are observed in the range 2.40−2.50 Å, depending on the axial ligand, whereas the metal−metal separation in dicopper tetracarboxylates ranges from 2.6 to 2.8 Å. The DFT/B3LYP calculations carried out in the present work on $Cu_3(dpa)_4Cl_2$ and $Cu_3(dpa)_4(BF_4)_2$ reproduce these intermetallic distances with good accuracy. Despite the shorter range of the Cu···Cu contacts imposed by the rigidity of the dpa coating, the electronic structure of the $(Cu_3)^{6+}$ species appears to be an extension to three metal centers of the orbital sequence now documented from various experimental and theoretical studies for carboxylato-bridged dinuclear Cu^{II} compounds. In both families of complexes, each metal atom generates a δ-type magnetic orbital whose lobes are directed toward the equatorial ligand environment with an antibonding character. In $Cu_3(dpa)_4Cl_2$, the antiferromagnetic coupling between consecutive metal atoms therefore involves a superexchange mechanism via the bridging dpa ligands. As for copper carboxylates, a contraction of the Cu···Cu distance tends to slightly *decrease* the exchange coupling parameter. Calculations on $Cu_3(dpa)_4(BF_4)_2$ confirm the latter point, and therefore do not explain the origin of the observed enhancement of the magnetic coupling with Cu···Cu contraction. By contrast, J should be extremely sensitive to any factor influencing the overlap spin population between metal and nitrogen. The 40% increase of the M−N negative overlap population associated with the magnetic orbitals upon substitution of Cu by Ag therefore accounts for the computed value of $-2J$ being multiplied by a factor of 3, from 436 to 1270 cm^{-1}. Oxidation of $M_3(dpa)_4Cl_2$ (M = Cu, Ag) eliminates the $(M-N_4)_{inner}$ moiety as a magnetic center. An antiferromagnetic interaction with calculated $-2J$ values of 64 cm^{-1} with copper (observed = 34 cm^{-1}) and 265 cm^{-1} with silver connects the terminal MN_4 fragments, following the same ligand pathways as for the neutral molecule. The strength of this interaction is correlated with the spin-polarized population of the x^2-y^2 orbital of the inner metal, which represents the crossing point of the four ligand pathways connecting the two magnetic centers. These antiferromagnetic interactions notwithstanding, no direct metal−metal bonding can be seen for $Cu_3(dpa)_4Cl_2$, $Ag_3(dpa)_4Cl_2$, and their oxidized counterparts. This is at variance with all symmetric $M_3(dpa)_4L_2$ investigated up to now, which all display some sort of delocalized bonding along the metal framework. Regardless of the relative strength of such bonds, their formal multiplicity could be graded as Cr > Co > Ni,

as far as neutral symmetric species are concerned. This order correlates with the response intensity of neutral $M_3(dpa)_4(NCS)_2$ species (M = Cr, Co, Ni) to STM stimulation, which is expected to measure the ability of individual molecules to transfer electrons.[16] It can therefore be expected that Cu^{II} or Ag^{II} metal chains, as their oxidized counterparts, should display the lowest capability to transfer electrons as compared with equivalent chain complexes involving less electron-rich transition metals.

Acknowledgment. We are grateful to the CNRS for support. Calculations have been shared between the IDRIS and the CINES National Computer Centers (Orsay and Montpellier, France) and the Centre Universitaire et Régional de Ressources en Informatique (ULP, Strasbourg, France). X.L. is grateful to the Government of Spain for a postdoctoral fellowship (EX-2004-0113).

Supporting Information Available: Bonding energies, Cartesian coordinates, atomic charges (Mulliken), and atomic spin populations corresponding to the optimal geometries calculated for the antiferromagnetic ground states, approximated by the broken-symmetry (BS) solutions, of $[M_3(dpa)_4Cl_2]^{0/+}$ (M = Cu, Ag) and $Cu_3(dpa)_4(BF_4)_2$. This material is available free of charge via the Internet at http://pubs.acs.org.

IC051799O